

Metabolic Youth in Middle Age: Predicting Aging in *Caenorhabditis elegans* Using Metabolomics

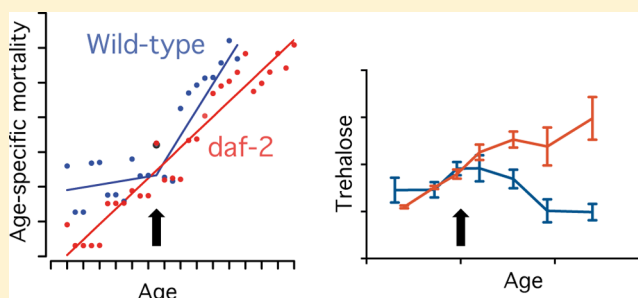
Sarah K. Davies,^{†,‡} Jacob G. Bundy,^{*,‡} and Armand M. Leroi^{*,†}

[†]Department of Life Sciences and [‡]Department of Surgery and Cancer, Imperial College London, Sir Alexander Fleming Building, London SW7 2AZ, U.K.

Supporting Information

ABSTRACT: Many mutations and allelic variants are known that influence the rate at which animals age, but when in life do such variants diverge from normal patterns of aging? Is this divergence visible in their physiologies? To investigate these questions, we have used ¹H NMR spectroscopy to study how the metabolome of the nematode *Caenorhabditis elegans* changes as it grows older. We identify a series of metabolic changes that, collectively, predict the age of wild-type worms. We then show that long-lived mutant *daf-2(m41)* worms are metabolically youthful compared to wild-type worms, but that this relative youth only appears in middle age. Finally, we show that metabolic age predicts the timing and magnitude of differences in age-specific mortality between these strains. Thus, the future mortality of these two genotypes can be predicted long before most of the worms die.

KEYWORDS: metabolomics, *daf-2*, trehalose, mortality



INTRODUCTION

Is it possible to predict the length of life remaining for any one individual? Some have suggested so;¹ however, there are substantial technical impediments. However, it is not unrealistic to predict the *probable* lifespan remaining at different points in life—the basis of the actuarial industry. Can this statistical approach be informed by the biological signature of an organism—can it increase the precision of these estimates? There are two obvious sources of information which might do so: personalized genomic data and phenotypic data, and it is likely that they will be especially powerful in combination. Here, we investigate this possibility by combining genetic with metabolic phenotypic data.

The untargeted profiling of small-molecule metabolites (metabolomics) gives an alternative measure of biochemical phenotype. This gives arguably the most direct phenotypic measurement at a cellular level: it integrates the complex upstream effects of regulation at transcriptional, translational, and post-translational levels.² In addition, and unlike genomic profiling, metabolomics is able to report on the combined effects of both genotype and environment (e.g., different dietary choices); this forms the basis of the so-called “pharmacometabonomic” or “pharmacometabolomic” approach, in which metabolic profiles are used to predict the response to drugs, integrating both genetic and environmental factors.^{3–5}

Caenorhabditis elegans has a relatively short lifespan of around 2–3 weeks (depending on temperature and food availability), which makes it an ideal model for the study of aging. Additionally, many single gene mutations have been found to

increase the lifespan of *C. elegans*. Many of these genes are components of the insulin/IGF-1-like signaling pathway and act via the transcription factor DAF-16 to activate genes associated with protection against oxidative stress and heat shock, those linked with autophagy and innate immunity, as well as other genes associated with survival.⁶ The *daf-2* gene is an orthologue of the human insulin receptor gene and is essential in *C. elegans*. However, certain hypomorphic mutations of *daf-2* increase lifespan; the amount of lifespan extension is variable between different mutants and depends on the environment, but *daf-2* lifespan can be as much as double that of wild-type.^{7,8}

As a phenomenon, aging clearly has many metabolic components. Longevity pathways are associated with specific metabolic enzymes, with many metabolism-linked genes activated by DAF-16.^{9–11} Wild-type worms have an abundance of proteins involved with lipid transport and translation elongation greater than that of *daf-2* worms, while these mutants have a comparatively high abundance of proteins involved in the biosynthesis of amino acids and the metabolism of reactive oxygen species, as well as those involved with carbohydrate metabolism.¹² Longevity-associated pathways have also been linked with key regulators of metabolism in *C. elegans*. The ratio of AMP to ATP is a measure of energy availability, and this ratio increases with age and changes in response to environmental stress. In worms, the AMP-activated protein kinase subunit AAK-2 acts as a sensor, being activated by AMP. Both environmental stress and reduced insulin

Received: May 20, 2015

Published: September 18, 2015

signaling have been found to increase longevity via AAK-2, which acts in parallel to DAF-16 to control lifespan.¹³ In addition to this, long-lived dauer larvae are known to have altered metabolism, as reviewed by Braeckman et al.,¹⁴ with a decreased metabolic rate and a reliance on lipids as a primary energy reserve rather than the combination of lipid and carbohydrate metabolism observed in non-dauer worms.

Given this, it is not surprising that recent studies have used metabolomic profiling to directly study the phenotypic changes that occur during aging.^{15–19} Previous metabolomic studies with *C. elegans* have focused on mutant comparisons rather than the aging process per se.^{20–24} We have previously analyzed metabolic changes during development;²⁵ here, we have used nuclear magnetic resonance (NMR) spectroscopy in an untargeted analysis of the metabolic changes that take place during the aging process, both in the wild-type and in a long-lived IIS mutant strain, and compared these to the mortality rate observed at different points in the life cycle.

MATERIALS AND METHODS

C. elegans Strains and Cultivation

We obtained worm strains (wild-type N2 and *daf-2(m41)*) from the Caenorhabditis Genetics Center (CGC). We maintained them at 20 °C on *Escherichia coli* OP50 on nematode growth medium (NGM (17 g L⁻¹ agar, 3 g of NaCl, 2.5 g of peptone, 1 mM CaCl₂, 1 mM MgSO₄, 25 mM K₂HPO₄ (pH 6), 0.1% cholesterol)). For the metabolite analysis, we synchronized the worms by hypochlorite treatment: bleaching solution (20% NaOCl (4%), 5% 10 M NaOH) was added to a pellet of gravid adults. After shaking and centrifugation, the pellet was washed with M9 buffer (22 mM KH₂PO₄, 42 mM Na₂HPO₄, 85.5 mM NaCl, 1 mM MgSO₄) and then transferred to a fresh NGM. When the worms reached young adulthood (defined as the point where there were eggs seen on the plates but no second-generation worms had hatched), they were transferred to plates containing 100 mg L⁻¹ fluorodeoxyuridine, in order to inhibit the growth of offspring so that all samples came from age-synchronous populations. We sampled them at young adulthood (60 h posthatch (p.h.) for N2 and 80 h p.h. for *daf-2(m41)*) and then at 6, 8, 10, 13, 16, and 20 days p.h. After 10 days, the worms were moved to fresh plates, and food (*E. coli* OP50 culture) was added regularly. We combined the worms from three individual 9 cm agar plates to make a single replicate (n = from 3 to 6). We sampled the worms by washing the plates in M9 buffer, allowing them to settle for 3 min, and aspirating off the supernatant. The pellets were snap-frozen and stored until metabolite analysis.

Survival Analysis

Worms were grown up following the protocol above, except that from young adulthood, they were kept 20 individuals per plate; we then monitored their survival until death (total numbers following censoring: n = 355 for wild-type and n = 352 for *daf-2(m41)*).

Metabolite Analysis

We extracted metabolites following the method described by Geier et al.²⁶ Briefly, the frozen pellets were extracted directly into ice-cold 80% methanol by bead-beating using 1 mm zirconia beads with a Precellys Dual (Cepheid, UK), and the extracts were dried under reduced pressure. The dried extracts were then resuspended in 0.65 mL of NMR buffer (0.1 M phosphate pH 7.0 and 0.97 mM sodium trimethylsilyl-²H₄-

propionate (TSP), in 100% ²H₂O), centrifuged (10 min, 16 000g), and 0.6 mL of the supernatant transferred to a 5 mm NMR tube. The TSP served as an internal frequency standard, and the ²H₂O both provided a field frequency lock for the spectrometer and helped reduce the signal from water. We analyzed the samples by ¹H NMR spectroscopy, using an Avance II DRX800 spectrometer equipped with a 18.2 T triple-resonance inverse cryoprobe with a proton resonance frequency of 800 MHz. The samples were held at 300 K during acquisition. We acquired 1D spectra essentially as described by Beckonert et al.²⁷ Briefly, we used the first line of a NOESY experiment for water suppression, and 256 scans per sample, with a recycle time of 5 s per scan. We processed the data in NMR Suite (Chenomx, Edmonton, Canada) and manually corrected each spectrum for phase and baseline. We then fitted 33 metabolites to every spectrum using the proprietary software library; all metabolites were present except for trehalose, which we added to the library. Probabilistic quotient normalization²⁸ was carried out on the data before analysis.

RESULTS

Genotype-Dependent and Genotype-Independent Metabolic Differences Associated with Aging

To investigate how the *C. elegans* metabolome ages, we studied the wild-type strain, N2, and a long-lived mutant, *daf-2(m41)*. DAF-2 encodes an insulin receptor that regulates life expectancy via the FOXO transcription factor, DAF-16.^{7,29} We sampled populations of synchronized wild-type and *daf-2(m41)* worms at seven ages: first, as young adults—2.5 days after hatching for N2 and 3.5 for *daf-2(m41)*, taking into account the latter's slower development—and then at days 6, 8, 10, 13, 16, and 20 after hatching. Using proton NMR spectroscopy, we identified 33 metabolites and estimated their pool sizes (Table S1). An unsupervised analysis (principal components) was difficult to interpret, as both genotype- and age-related differences were visible on the same axes (Supporting Information, Figure S1). We therefore used a supervised approach to help separate out the different effects: orthogonal projections to latent structures (O-PLS) can be used to model factors in a supervised fashion but has the additional benefit that an extra and effectively unsupervised axis (or axes) can be extracted.³⁰ This demonstrates that the strains are clearly metabolically distinct (the model is supervised with respect to genotype, i.e., correlated component); in addition, there is a strong effect of age on metabolite profiles, such that both strains map to an unsupervised “age” axis (orthogonal component) once the effects of genotype are allowed for (Figure 1). We then went on to examine the behavior of individual metabolites using linear models and found that 26 of them showed clear age-specific responses, that is, linear changes in pool size with age in either genotype (p < 0.05, Figure 2A); 15 of these metabolites had significantly different gradients between the genotypes (p < 0.05).

Surveying our metabolites, we found that DAF-2 modified their age-specific responses in one of three ways. We used these responses to classify them. The first (class A) consists of metabolites that show a large change with age in wild-type worms but no change or only a modest change in *daf-2* worms (Figure 2B,i,ii): putrescine, serine, and citrate increase with age in wild-type worms and show little or no change in *daf-2* worms. The second (class B: phosphocholine, leucine, valine,

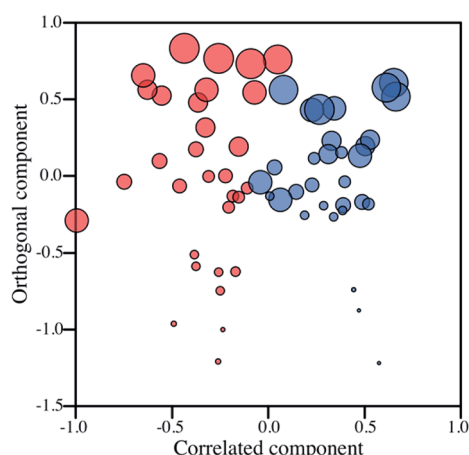


Figure 1. Metabolic effect of aging visible for both strains. Orthogonal PLS discriminant analysis of genotype, using log-transformed and mean-centered data, with one correlated and one orthogonal component; here, the analysis is supervised with respect to strain (correlated component) but unsupervised with respect to age (orthogonal component). Wild-type, blue; *daf-2(m41)*, red. Circle size corresponds to age. Model statistics: $R^2Y = 0.737$, $Q^2Y = 0.668$.

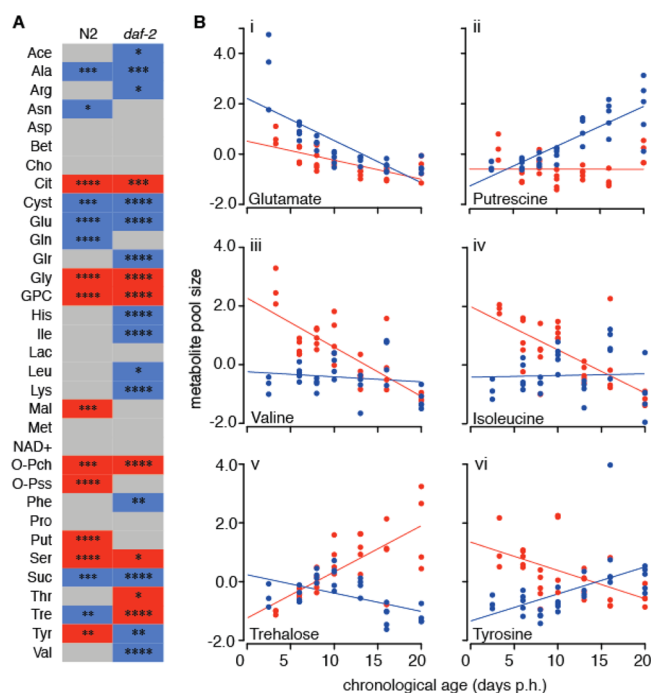


Figure 2. (A) Linear changes in metabolite pool size in wild-type and *daf-2* worms. Linear increases with age are shown in red; linear decreases are in blue. Metabolites with pool sizes not significantly fitting a linear model are shown in gray. * $P < 0.05$; ** $P < 0.01$; *** $P < 0.001$; **** $P < 0.0001$. (B) Age responses in selected metabolites: (i,ii) metabolites that show a large change with age in wild-type worms but no change or only a modest change in *daf-2* worms; (iii,iv) metabolites that show little/no change in wild-type worms but a large change in *daf-2* worms; (v,vi) metabolites showing opposite responses in wild-type and *daf-2* worms. Pool sizes have been averaged, and unit variance has been standardized. Wild type, blue; *daf-2(m41)*, red.

isoleucine, cystathionine, phenylalanine, histidine, glycerol) consists of those that show little or no change in wild-type worms but a large change in *daf-2* worms (Figure 2B,iii,iv). All but phosphocholine decrease with age in *daf-2* worms. The

third class of metabolites (class C: trehalose, tyrosine) have opposite responses in wild-type and *daf-2* worms (Figure 2B,v,vi).

Predictive Modeling of Age

The results show that there were, indeed, clear age-related effects on metabolism (Figure 1). To see if these metabolic differences were sufficient to predict the age of worms, we carried out a partial least-squares (PLS) regression of metabolite pool size on age separately for each genotype, using all 33 metabolites. In each case, we were able to construct robust models (Figure 3A,B). Thus, metabolite concentrations alone are excellent predictors of the chronological age of a population of worms. Metabolites that predict chronological age in one genotype need not, however, do so in another. This is shown by the loadings of the metabolites for the different PLS models: as might be expected, class A metabolites (e.g., putrescine) load most strongly on the wild-type model, while class B metabolites (e.g., valine) load on the *daf-2* model; class C metabolites load on both (Figure 3C).

Can we predict the relative “metabolic age” of our genotypes, that is, what results do the *daf-2* data give when applied to the wild-type model? If the metabolome is causally linked to aging resistance, then *daf-2* worms should be metabolically younger than wild-type at some, or even all, chronological ages. To examine this, we fitted the *daf-2(m41)* metabolome data to the wild-type model and vice versa (Figure 3A,B). We found that both models show that *daf-2* is metabolically younger than wild-type for part of the adult life. However, the two models disagree when *daf-2(m41)* acquires resistance to aging. The wild-type model predicts that *daf-2* worms only acquire their relative youth in middle age, around 15 days p.h. The *daf-2* model, on the other hand, predicts that the wild-type worms are “metabolically older” than *daf-2* worms in early life, but the two strains then converge. These divergent predictions clearly stem from the fact that different metabolites contribute to each model. Which, if either, is right?

daf-2(m41) Worms Become Aging-Resistant in Middle Age

To discriminate between these two models, which we can call “early-” versus “late-life” aging resistance, we investigated the age-specific mortality of these genotypes. The most commonly used model of aging, the Gompertz aging function, assumes that the age-specific mortality rate, μ_x , can be decomposed into two components, an age-independent mortality rate, a , and an exponentially increasing age-dependent mortality rate, b .

$$\mu_x = a^{(bx)}$$

If mortality rate is plotted against age on a semilogarithmic plot, this implies a linear relationship, in which x is age, the intercept is a , and the slope b , the last of which is generally held to represent the “rate of aging”.³¹ If worm aging is adequately described by this function and if long-lived mutants do, indeed, have increased resistance to aging, then they should have a b lower than that in wild-type worms. However, studies in many organisms, including *C. elegans*, have shown that the rate of aging can vary over the course of life;^{31,32} thus the dynamics of aging may be more complicated than allowed by a simple Gompertz model.

Many longevity assays of *daf-2* mutants have been carried out, but few have attempted to estimate age-specific mortality rates. To estimate b , we assayed the longevity in a large population of worms and fitted one- and two-stage Gompertz models to the data; in the latter, maximum likelihood estimates

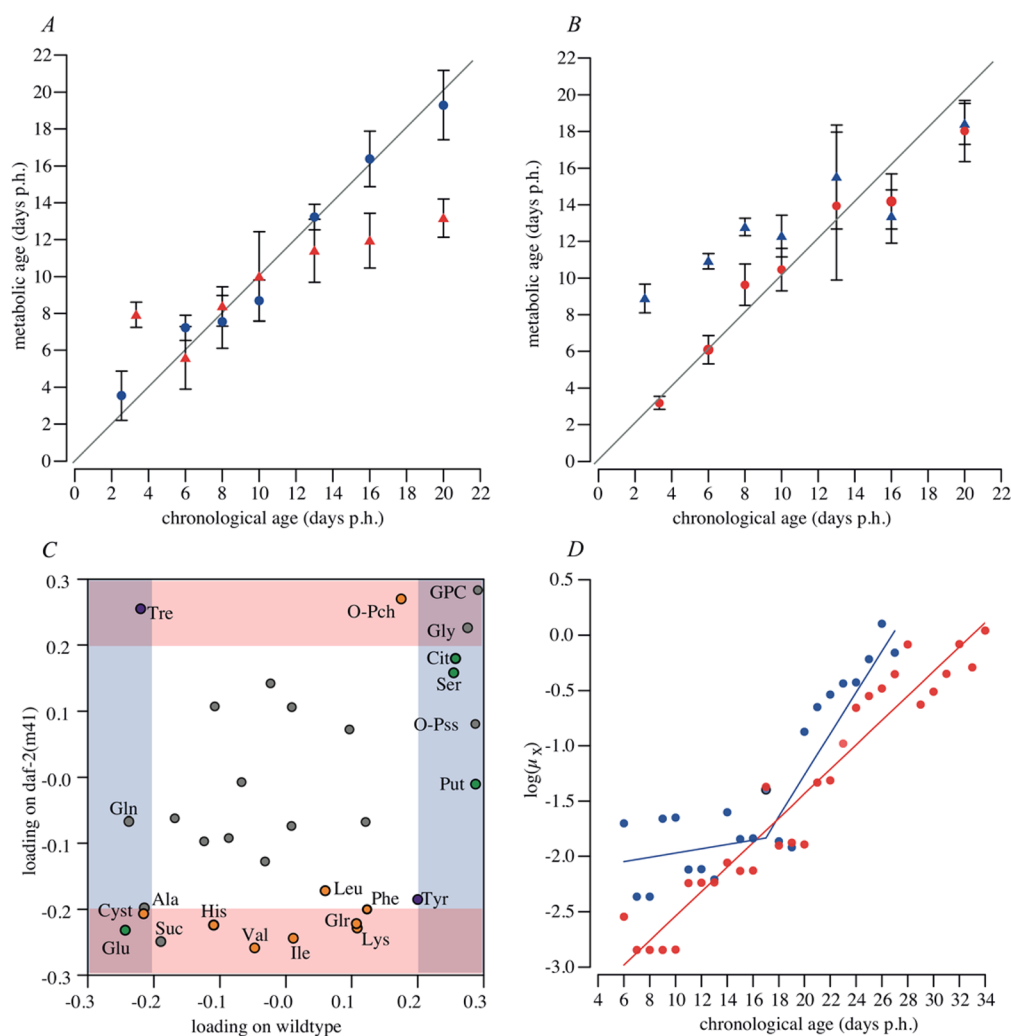


Figure 3. (A) PLS model based on wild-type (blue circles) with *daf-2(m41)* data fitted (red triangles). (B) PLS model based on *daf-2(m41)* (red circles) with wild-type data fitted (blue triangles). Gray lines show a perfect fit ($x = y$). Both models show that *daf-2* is “metabolically younger” than wild-type at some point in its life but at different time points. (C) Metabolite loadings on PLS models. Wild-type high-loading region in blue; *daf-2(m41)* high-loading region in red; combined in purple. Amino acids are designated with standard three-letter codes; the remainder are citrate (Cit), glycerol (Glr), O-phosphocholine (O-Pch), O-phosphoserine (O-Pss), putrescine (Put), succinate (Suc), *sn*-glycero-3-phosphocholine (GPC), and trehalose (Tre). Class A metabolites, green; class B, orange; class C, purple; no response, or genotype-indistinguishable response, gray. (D) Age-specific mortality of wild-type (blue) and *daf-2(m41)* (red). Lines represent Gompertz fits; the rate of aging is their slope, b . The best fit to the wild-type pattern of mortality is a two-stage Gompertz with a break at 17.5 days posthatch; in *daf-2(m41)*, no such break is required, with the result that in early adulthood it ages faster and in late life slower than wild-type.

of the parameters and break point are given by segmented linear regression.³³ For wild-type, we found that a two-stage model fitted the data significantly better than a one-stage model ($p = 0.0007$, two-sided Davies test) with a break at 17.5 days (95% confidence intervals: 12.8–19.6 days) and a sharp (10-fold) increase in the rate of aging after the break: $b_{WT,1} = 0.019$ (−0.043; 0.082) and $b_{WT,2} = 0.186$ (0.123; 0.249). By contrast, we found that for *daf-2(m41)* a two-stage model was not justified ($p = 0.3$, two-sided Davies test), so we fitted a one-stage Gompertz: $b_{daf-2} = 0.110$ (0.099; 0.121). The difference between these slopes is significant ($b_{WT,1}$ vs $b_{daf-2} = p = 0.0003$; $b_{WT,2}$ vs $b_{daf-2} = p = 0.0003$, ANCOVA) and shows that after the middle age break-point *daf-2(m41)* worms age about 40% slower than wild-type worms, but that younger worms age about 6-fold faster. Thus, it appears that the dynamics of aging in wild-type and *daf-2(m41)* worms are very different, and that *daf-2(m41)*’s resistance to aging is acquired in middle age (Figure 3D). This pattern of relative age-specific mortality is

precisely that predicted by the wild-type model but is very different from the *daf-2* model. That, in turn, suggests that class A metabolites predict biological age but that class B metabolites do not.

DISCUSSION

We do not know the functional significance of these metabolite classes but speculate that, if there are metabolites that have a causal role in contributing to increased longevity, they would have patterns like class B or C metabolites; that is, they would be significantly altered in long-lived worm strains but not in wild-type, or they would have opposite responses in long-lived and wild-type strains. For example, in an earlier study, we showed that the branched chain amino acids (BCAAs), isoleucine, leucine, and valine, are elevated in young adult *daf-2* worms;²³ here, we confirm that result but also show that they are class B metabolites in that they converge to wild-type levels later on. Since BCAAs are among the few DAF-2-

regulated metabolites that require DAF-16²³—the classical test⁸—they are strong candidates for being causally involved in resistance to aging. Indeed, dietary BCAAs increase the lifespan of mice when first introduced to their diet in middle age.³⁴ BCAAs also increase wild-type *C. elegans*’ lifespan when introduced as a dietary supplement from hatching, although nearly all amino acids were reported to have similar effects on lifespan under specific growth conditions.³⁵ We previously found that trehalose was upregulated in some *daf-2* mutants when they were young adults but not *m41*; here, we find that it is a class C metabolite that decreases strongly after middle age in N2 worms but increases in *daf-2(m41)*, so that by day 20, *daf-2(m41)* worms have about 3-fold as much trehalose as N2 (Figure S2). Again, this is consistent with lifespan-extending effects reported in the literature: trehalose increases lifespan in *C. elegans*, and feeding N2 worms trehalose during early adulthood does not increase lifespan but feeding them in middle age does increase their lifespan.³⁶ Trehalose addition does not extend the lifespan of *daf-2* worms,³⁶ and as the *daf-2*-related difference appears strongly only from middle age, it may be that because *daf-2* worms have high trehalose already, the extra trehalose does not have an effect.

It is important to note that our analysis of 33 metabolites is based on linear models. If pool sizes change in a nonlinear way with age—and it is likely that they do—then our analysis will tend to underestimate the amount of regulation. Additionally, it is not necessarily the case that the metabolite changes observed in *daf-2(m41)* worms would occur in other *daf-2* alleles or in other long-lived mutants. Profiling the aging process in double mutants would provide yet further information; for example, *daf-2;daf-16* is a classic example of an epistatic interaction where the lifespan extension is reversed by the presence of the second mutation.³⁷ We have previously identified *daf-16*-dependent metabolic changes as a subset of *daf-2*-caused changes at a single time point.²³ While we have shown that this type of study is a potentially useful way to generate testable hypotheses, clearly further experiments are required to investigate the functional link between mortality rate and metabolic profile.

We have previously reported that the use of 5'-fluorodeoxyuridine (FUDR) may have a genotype-specific effect on the levels of some metabolites,³⁸ but collecting the biomass of worms required for this analysis would not have been possible without the use of FUDR or similar intervention. Eight metabolites previously found to have levels affected by an interaction between FUDR and genotype were included in this study. Of these, betaine, lactate, and NAD do not increase or decrease significantly with age in either strain in this data set, and despite a more pronounced change in the presence of FUDR, levels of glycerol and tyrosine were found at levels in *daf-2* lower than those of N2 worms under both conditions. However, we recognize that caution should be used when interpreting data for the three remaining metabolites; glutamate and glutamine levels were lower in *daf-2* than in N2 without FUDR, but this change was reversed when grown on FUDR-containing medium, and differences in GPC levels between strains only existed in the presence of FUDR.

This study highlights the importance of evaluating multiple time points in wild-type/mutant comparisons; given the differences in the metabolic changes that occur with age in the two strains, reporting absolute differences between genotypes at only one time point may not be sufficient to characterize metabolic changes of interest. Previously, we used

NMR-based metabolomics to compare the metabolic effects of several longevity mutants, including *daf-2(m41)*, but this was only at a single time point.²³ Pontoizeau et al.³⁹ compared wild-type worms with long-lived dietary restriction mutants at two time points (also using FUDR to inhibit reproduction): young adulthood and day 7 of adulthood, reporting similar changes in pool sizes with age in wild-type worms for several metabolites including alanine, phosphocholine, and GPC. The pool size changes of some metabolites, including leucine and trehalose, were also consistent across long-lived mutants in both studies.

Thus, we conclude that (1) worms commence aging in middle age; and (2) metabolites that are strongly correlated with aging in wild-type worms but not in this *daf-2* mutant (class A) or are divergently regulated (class C) can be used to accurately predict this pattern of aging. It has long been known that individuals with different genotypes have different life expectancies. This is true of mutant worms, and it is true of natural genetic variance in humans.^{40–42} In addition, experiments on single genotypes have shown that it is possible to predict longevity for individuals based on the expression levels of specific genes.⁴³ However, life expectancy is a very crude measure of mortality. It provides no information on the pattern of age-specific mortality—it just tells you that one genotype lives longer or shorter than another. Indeed, a difference in life expectancy need not be due to a difference in the rate of aging at all, as opposed to a difference in the age-independent rate of death. It is clear, however, that the ability to predict the age-dependent rate of mortality and morbidity (which is highly correlated with mortality) would be of extraordinary medical and social value. Our results provide a first step to showing that different genotypes have different patterns of age-specific mortality that can be predicted by metabolomic markers. We expect that the combination of genetic and metabolomic data will in the future be powerful tools in managing an aging population.

■ ASSOCIATED CONTENT

§ Supporting Information

The Supporting Information is available free of charge on the ACS Publications website at DOI: 10.1021/acs.jproteome.5b00442.

Supplementary figures and table (PDF)

■ AUTHOR INFORMATION

Corresponding Authors

*E-mail: j.bundy@imperial.ac.uk.

*E-mail: a.leroi@imperial.ac.uk.

Notes

The authors declare no competing financial interest.

■ ACKNOWLEDGMENTS

This study was supported by the Natural Environment Research Council (NERC), U.K.

■ REFERENCES

- (1) Heinlein, R. A. Life-line. *Astounding Science-Fiction* 1939, 23.
- (2) Raamsdonk, L. M.; Teusink, B.; Broadhurst, D.; Zhang, N. S.; Hayes, A.; Walsh, M. C.; Berden, J. A.; Brindle, K. M.; Kell, D. B.; Rowland, J. J.; Westerhoff, H. V.; van Dam, K.; Oliver, S. G. A functional genomics strategy that uses metabolome data to reveal the phenotype of silent mutations. *Nat. Biotechnol.* 2001, 19, 45–50.

- (3) Clayton, T. A.; Lindon, J. C.; Cloarec, O.; Antti, H.; Charuel, C.; Hanton, G.; Provost, J. P.; Le Net, J. L.; Baker, D.; Walley, R. J.; Everett, J. R.; Nicholson, J. K. Pharmacometabonomic phenotyping and personalized drug treatment. *Nature* **2006**, *440*, 1073–1077.
- (4) Holmes, E.; Wilson, I. D.; Nicholson, J. K. Metabolic phenotyping in health and disease. *Cell* **2008**, *134*, 714–717.
- (5) Phapale, P. B.; Kim, S. D.; Lee, H. W.; Lim, M.; Kale, D. D.; Kim, Y. L.; Cho, J. H.; Hwang, D.; Yoon, Y. R. An integrative approach for identifying a metabolic phenotype predictive of individualized pharmacokinetics of tacrolimus. *Clin. Pharmacol. Ther.* **2010**, *87*, 426–436.
- (6) Gems, D.; Partridge, L. Genetics of longevity in model organisms: debates and paradigm shifts. *Annu. Rev. Physiol.* **2013**, *75*, 621–644.
- (7) Gems, D.; Sutton, A. J.; Sundermeyer, M. L.; Albert, P. S.; King, K. V.; Edgley, M. L.; Larsen, P. L.; Riddle, D. L. Two pleiotropic classes of *daf-2* mutation affect larval arrest, adult behavior, reproduction and longevity in *Caenorhabditis elegans*. *Genetics* **1998**, *150*, 129–155.
- (8) Kenyon, C.; Chang, J.; Gensch, E.; Rudner, A.; Tabtiang, R. A *C. elegans* mutant that lives twice as long as wild type. *Nature* **1993**, *366*, 461–464.
- (9) Halaschek-Wiener, J.; Khattra, J. S.; McKay, S.; Pouzyrev, A.; Stott, J. M.; Yang, G. S.; Holt, R. A.; Jones, S. J.; Marra, M. A.; Brooks-Wilson, A. R.; Riddle, D. L. Analysis of long-lived *C. elegans daf-2* mutants using serial analysis of gene expression. *Genome Res.* **2005**, *15*, 603–615.
- (10) Lee, S. S.; Kennedy, S.; Tolonen, A. C.; Ruvkun, G. DAF-16 target genes that control *C. elegans* life-span and metabolism. *Science* **2003**, *300*, 644–647.
- (11) Murphy, C. T.; McCarroll, S. A.; Bargmann, C. I.; Fraser, A.; Kamath, R. S.; Ahringer, J.; Li, H.; Kenyon, C. Genes that act downstream of DAF-16 to influence the lifespan of *Caenorhabditis elegans*. *Nature* **2003**, *424*, 277–283.
- (12) Dong, M. Q.; Venable, J. D.; Au, N.; Xu, T.; Park, S. K.; Cociorva, D.; Johnson, J. R.; Dillin, A.; Yates, J. R. Quantitative mass spectrometry identifies insulin signaling targets in *C. elegans*. *Science* **2007**, *317*, 660–663.
- (13) Apfeld, J.; O'Connor, G.; McDonagh, T.; DiStefano, P. S.; Curtis, R. The AMP-activated protein kinase AAK-2 links energy levels and insulin-like signals to lifespan in *C. elegans*. *Genes Dev.* **2004**, *18*, 3004–3009.
- (14) Braeckman, B. P.; Houthoofd, K.; Vanfleteren, J. R. Patterns of metabolic activity during aging of the wild type and longevity mutants of *Caenorhabditis elegans*. *J. Am. Aging Assoc.* **2000**, *23*, 55–73.
- (15) Houtkooper, R. H.; Argmann, C.; Houten, S. M.; Canto, C.; Jenjira, E. H.; Andreux, P. A.; Thomas, C.; Doenlen, R.; Schoonjans, K.; Auwerx, J. The metabolic footprint of aging in mice. *Sci. Rep.* **2011**, *1*, 134.
- (16) Son, N.; Hur, H. J.; Sung, M. J.; Kim, M. S.; Hwang, J. T.; Park, J. H.; Yang, H. J.; Kwon, D. Y.; Yoon, S. H.; Chung, H. Y.; Kim, H. J. Liquid Chromatography-Mass Spectrometry-based Metabolomic Analysis of Livers from Aged Rats. *J. Proteome Res.* **2012**, *11*, 2551–2558.
- (17) Swann, J. R.; Spagou, K.; Lewis, M.; Nicholson, J. K.; Glei, D. A.; Seeman, T. E.; Coe, C. L.; Goldman, N.; Ryff, C. D.; Weinstein, M.; Holmes, E. Microbial-Mammalian Cometalolites Dominate the Age-associated Urinary Metabolic Phenotype in Taiwanese and American Populations. *J. Proteome Res.* **2013**, *12*, 3166–3180.
- (18) Wang, Y.; Lawler, D.; Larson, B.; Ramadan, Z.; Kochhar, S.; Holmes, E.; Nicholson, J. K. Metabonomic investigations of aging and caloric restriction in a life-long dog study. *J. Proteome Res.* **2007**, *6*, 1846–1854.
- (19) Williams, R. E.; Lenz, E. M.; Lowden, J. S.; Rantalainen, M.; Wilson, I. D. The metabolomics of aging and development in the rat: an investigation into the effect of age on the profile of endogenous metabolites in the urine of male rats using 1H NMR and HPLC-TOF MS. *Mol. Biosyst.* **2005**, *1*, 166–175.
- (20) Jaeger, C.; Tellstrom, V.; Zurek, G.; Konig, S.; Eimer, S.; Kammerer, B. Metabolomic changes in *Caenorhabditis elegans* lifespan mutants as evident from GC-ESI-MS and GC-APCI-TOF-MS profiling. *Metabolomics* **2014**, *10*, 859–876.
- (21) Castro, C.; Sar, F.; Shaw, W. R.; Mishima, M.; Miska, E. A.; Griffin, J. L. A metabolomic strategy defines the regulation of lipid content and global metabolism by Delta9 desaturases in *Caenorhabditis elegans*. *BMC Genomics* **2012**, *13*, 36.
- (22) Castro, C.; Krumsiek, J.; Lehrbach, N. J.; Murfitt, S. A.; Miska, E. A.; Griffin, J. L. A study of *Caenorhabditis elegans* DAF-2 mutants by metabolomics and differential correlation networks. *Mol. Biosyst.* **2013**, *9*, 1632–1642.
- (23) Fuchs, S.; Bundy, J. G.; Davies, S. K.; Viney, J. M.; Swire, J. S.; Leroi, A. M. A metabolic signature of long life in *BMC Biol.* **2010**, *8*, 14.
- (24) Martin, F. P.; Spanier, B.; Collino, S.; Montoliu, I.; Kolmeder, C.; Giesbertz, P.; Affolter, M.; Kussmann, M.; Daniel, H.; Kochhar, S.; Rezzi, S. Metabotyping of *Caenorhabditis elegans* and their culture media revealed unique metabolic phenotypes associated to amino acid deficiency and insulin-like signaling. *J. Proteome Res.* **2011**, *10*, 990–1003.
- (25) Swire, J.; Fuchs, S.; Bundy, J. G.; Leroi, A. M. The cellular geometry of growth drives the amino acid economy of *Caenorhabditis elegans*. *Proc. R. Soc. London, Ser. B* **2009**, *276*, 2747–2754.
- (26) Geier, F. M.; Want, E. J.; Leroi, A. M.; Bundy, J. G. Cross-platform comparison of *Caenorhabditis elegans* tissue extraction strategies for comprehensive metabolome coverage. *Anal. Chem.* **2011**, *83*, 3730–3736.
- (27) Beckonert, O.; Keun, H. C.; Ebbels, T. M.; Bundy, J.; Holmes, E.; Lindon, J. C.; Nicholson, J. K. Metabolic profiling, metabolomic and metabonomic procedures for NMR spectroscopy of urine, plasma, serum and tissue extracts. *Nat. Protoc.* **2007**, *2*, 2692–2703.
- (28) Dieterle, F.; Ross, A.; Schlotterbeck, G.; Senn, H. Probabilistic quotient normalization as robust method to account for dilution of complex biological mixtures. Application in 1H NMR metabolomics. *Anal. Chem.* **2006**, *78*, 4281–4290.
- (29) Patel, D. S.; Garza-Garcia, A.; Nanji, M.; McElwee, J. J.; Ackerman, D.; Driscoll, P. C.; Gems, D. Clustering of genetically defined allele classes in the *Caenorhabditis elegans* DAF-2 insulin/IGF-1 receptor. *Genetics* **2008**, *178*, 931–946.
- (30) Trygg, J.; Wold, S. Orthogonal projections to latent structures. *J. Chemom.* **2002**, *16*, 119–128.
- (31) Johnson, T. E.; Wu, D.; Tedesco, P.; Dames, S.; Vaupel, J. W. Age-specific demographic profiles of longevity mutants in *Caenorhabditis elegans* show segmental effects. *J. Gerontol., Ser. A* **2001**, *56*, B331–9.
- (32) Chen, J.; Senturk, D.; Wang, J. L.; Muller, H. G.; Carey, J. R.; Caswell, H.; Caswell-Chen, E. P. A demographic analysis of the fitness cost of extended longevity in *Caenorhabditis elegans*. *J. Gerontol., Ser. A* **2007**, *62*, 126–135.
- (33) Muggeo, V. M. Estimating regression models with unknown break-points. *Stat. Med.* **2003**, *22*, 3055–3071.
- (34) D'Antona, G.; Ragni, M.; Cardile, A.; Tedesco, L.; Dossena, M.; Bruttini, F.; Caliaro, F.; Corsetti, G.; Bottinelli, R.; Carruba, M. O.; Valerio, A.; Nisoli, E. Branched-chain amino acid supplementation promotes survival and supports cardiac and skeletal muscle mitochondrial biogenesis in middle-aged mice. *Cell Metab.* **2010**, *12*, 362–372.
- (35) Edwards, C.; Canfield, J.; Copes, N.; Brito, A.; Rehan, M.; Lipps, D.; Brunquell, J.; Westerheide, S. D.; Bradshaw, P. C. Mechanisms of amino acid-mediated lifespan extension in *Caenorhabditis elegans*. *BMC Genet.* **2015**, *16*, 8.
- (36) Honda, Y.; Tanaka, M.; Honda, S. Trehalose extends longevity in the nematode *Caenorhabditis elegans*. *Aging Cell* **2010**, *9*, 558–569.
- (37) Ogg, S.; Paradis, S.; Gottlieb, S.; Patterson, G. I.; Lee, L.; Tissenbaum, H. A.; Ruvkun, G. The Fork head transcription factor DAF-16 transduces insulin-like metabolic and longevity signals in *C. elegans*. *Nature* **1997**, *389*, 994–999.
- (38) Davies, S. K.; Leroi, A. M.; Bundy, J. G. Fluorodeoxyuridine affects the identification of metabolic responses to *daf-2* status in *Caenorhabditis elegans*. *Mech. Ageing Dev.* **2012**, *133*, 46–49.

(39) Pontoizeau, C.; Mouchiroud, L.; Molin, L.; Mergoud-Dit-Lamarche, A.; Dalliere, N.; Toulhoat, P.; Elena-Herrmann, B.; Solari, F. Metabolomics analysis uncovers that dietary restriction buffers metabolic changes associated with aging in *Caenorhabditis elegans*. *J. Proteome Res.* **2014**, *13*, 2910–2919.

(40) Kent, J. W. J.; Goring, H. H.; Charlesworth, J. C.; Drigalenko, E.; Diego, V. P.; Curran, J. E.; Johnson, M. P.; Dyer, T. D.; Cole, S. A.; Jowett, J. B.; Mahaney, M. C.; Comuzzie, A. G.; Almasy, L.; Moses, E. K.; Blangero, J.; Williams-Blangero, S. Genotypexage interaction in human transcriptional ageing. *Mech. Ageing Dev.* **2012**, *133*, 581–590.

(41) Uciechowski, P.; Oellig, E. M.; Mariani, E.; Malavolta, M.; Mocchegiani, E.; Rink, L. Effects of human Toll-like receptor 1 polymorphisms on ageing. *Immun. Ageing* **2013**, *10*, 4.

(42) Willcox, B. J.; Donlon, T. A.; He, Q.; Chen, R.; Grove, J. S.; Yano, K.; Masaki, K. H.; Willcox, D. C.; Rodriguez, B.; Curb, J. D. FOXO3A genotype is strongly associated with human longevity. *Proc. Natl. Acad. Sci. U. S. A.* **2008**, *105*, 13987–13992.

(43) Pincus, Z.; Smith-Vikos, T.; Slack, F. J. MicroRNA predictors of longevity in *Caenorhabditis elegans*. *PLoS Genet.* **2011**, *7*, e1002306.